ON THE DESIGN OF AN FBMC BASED AIR INTERFACE ENABLING CHANNEL ADAPTIVE PULSE SHAPING PER SUB-BAND

Martin Fuhrwerk and Jürgen Peissig

Malte Schellmann

Institute of Communication Technologies
Leibniz Universität Hannover
{fuhrwerk,peissig}@ikt.uni-hannover.de

Huawei European Research Center
Munich
malte.schellmann@huawei.com

ABSTRACT

By application of pulse shaping, the FBMC (Filter Bank Multi Carrier) based offset-QAM-OFDM (OQAM-OFDM) modulation scheme offers a new degree of freedom in designing mobile communication systems. In this contribution we investigate the coexistence performance in terms of interference isolation of individually configured sub-bands, i.e. individual prototype filter functions (PFF) and/or subcarrier spacing per sub-band, in the context of multi-user or multi-service scenarios as envisaged for 5G. To that end, we analyze the synchronization requirements of different of PFF from literature suggested for OQAM-OFDM and determine the required amount of guard bands with respect to the applied PFFs and subcarrier spacing configurations. The simulation results prove that the required amount of guard bands for OQAM-OFDM systems is independent on the time offset between different users. As a rule of thumb we can state, that for a minimum co-user interference isolation of 20 dB a bandwidth of one subcarrier spacings of the user with the largest subcarrier spacing has to be used as in-band guard bands.

Index Terms— OQAM-OFDM, Pulse shaping, Prototype filter, FBMC, Coexistence, MTC

1. INTRODUCTION

Most of the nowadays mobile communication systems are single-service systems based on Cyclic-Prefix OFDM (CP-OFDM), e.g. LTE, DVB-T and WiFi. This modulation scheme is not the perfect match for multi-service scenarios as envisaged for the upcoming mobile communication standard 5G. Due to the inherent rectangular pulse shaping, CP-OFDM suffers from high co-user/co-service interference in case synchronization in time and/or frequency cannot established perfectly. This leads to the need for a large amount of guard bands between users/services to enable coexistence. In MTC scenarios, which are as well intended to be covered by 5G, it is not beneficial to keep users strictly synchronized, since typical machine type devices are supposed to transmit with very low duty cycles in the range of several seconds up to minutes or hours without being always connected to the network, to save signaling overhead and therefor to extend battery lifetime [1].

To enhance the coexistence capabilities of the complete system design, a modulation scheme better spectral containment of the signals is advised. One promising candidate to achieve a high overall spectrum occupancy which is discussed in literature is the FBMC based OQAM-OFDM. In contrast to CP-OFDM it enables the usage of PFF, which can be designed to reduce the side lobes of the spectra and thus improve the coexistence capabilities of a communication system with adjacent or in-band interferer [2]. Additionally, the flexibility of the FBMC structure enables full adaptivity of waveform and transceiver design responding to any kind of requirements given by a service or application [3].

Recent studies proved that the theoretically predicted performance gains obtained by channel adaptive pulse shaping translate to considerable SIR improvements in practical scenarios [4]. In this work, we investigate the influence of channel adaptive modulation on the interference isolation in the context of multi-user or mixed-service scenarios. Therefore, we analyze the coexistence performance of individually configured sub-bands under consideration of PFFs from literature suggested for OQAM-OFDM and determine the required amount of guard bands with respect to the applied PFFs and subcarrier spacing configurations as depicted in Figure 1.

The rest of the paper is organized as follows. In section 2 the applied OQAM-OFDM system model is introduced, followed by the description of the modeling of interference between coexisting systems with different configurations in section 3. The simulation results are discussed in section 4. Finally the main outcome is summarized in the conclusion.

2. SYSTEM MODEL

In this section, we first provide a description of the system model followed by the derivation of the co-user interference in dependence on time and frequency synchronization offsets as well as the size of in-band guard bands. This work
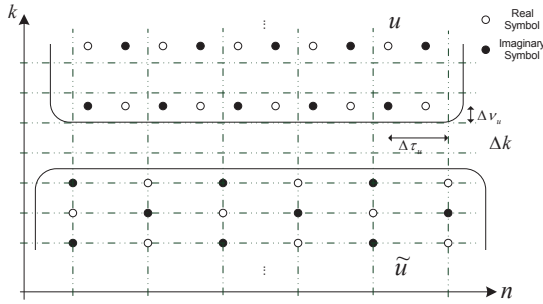
Fig. 1. Time-frequency plane schematic for the coexistence of two non-synchronized OQAM-OFDM systems utilizing different subcarrier spacings. Thereby user u has twice the subcarrier spacing of user $\tilde{u}$.

merely focuses on the influence of the co-user interference of OQAM-OFDM systems and thus receiver noise is neglected in our investigation. Accordingly, the time-discrete system model considered in this paper is described by

$$r[n] = \sum_{u \in \mathbb{U}} h_u[n] * s_u[n], \qquad (1)$$

whereby the received signal $r[n]$ at sample index n is an aggregation of $U = |\mathbb{U}|$ active user specific transmit signals $s_u[n]$, passing through user specific channels with impulse response $h_u[n]$. The applied lattice grid in relation to the symbol duration K_u is defined by τ_0 and ν_0, where τ_0 and ν_0 are the normalized symbol duration and subcarrier spacing, respectively. Here, these parameters are set to $\tau_0 = 0.5$ and $\nu_0 = 1$. For an OQAM-OFDM system utilizing a total number of $K_u \in \mathbb{N}$ subcarriers with $\exists K_u : \tau_0 K_u \notin \mathbb{N}$, the oversampled transmit signal $s_u[n]$ for the u-th user is given by

$$s_u[n] = \sum_{(m,k)} \theta_{m,k} d^u_{k,m} p^u_k[n - mK_u] \qquad (2)$$

where $d_{k,m}$ is a real-valued OQAM symbol mapped to subcarrier $k \in \mathbb{K}_u$ of the FBMC symbol with time index $m \in \mathbb{M}_u$ and $\theta_{m,k} = j^{m+k}$ represents the phase shift required to establish the real orthogonality at the receiver for OQAM-OFDM in the time-frequency plane. $\mathbb{K}_u \subseteq \{0, 1, \ldots, K-1\}$ indicates the set of subcarriers allocated by user u and $\mathbb{M}_u$ the set of allocated FBMC symbols, respectively. $p^u_k[n]$ is the user specific real valued and symmetric PFF modulated at subcarrier k according to

$$p_k[n] = p[n] e^{-j2\pi\tau_0\nu_0 k \frac{n}{K_u}}. \qquad (3)$$

As mentioned before users may have different subcarrier spacings. To unify the user specific lattice grids a joint virtual lattice grid with K virtual subcarriers is introduced for all users, where $\forall K_u : K/K_u \in \mathbb{N} \wedge K_u \varepsilon_u = K$ holds. Thereby ε_u is the user specific oversampling factor in frequency domain.

In our investigation each user is subject to a propagation delay $\tau_u \in \mathbb{R} \wedge \tau_u K \in \mathbb{Z}$ normalized to the joint virtual symbol duration K and a carrier frequency offset (CFO) $\nu_u \in \mathbb{R}$ normalized to the joint virtual subcarrier spacing caused by oscillator imperfections, respectively. The user specific channel impulse response $h_u[n]$ is defined by

$$h_u[n] = \delta[n - \tau_u K] e^{-j\pi\nu_u \frac{n}{K}}. \qquad (4)$$

With the symmetry properties of the PFFs the received real OQAM symbols $\tilde{d}_{\tilde{k},\tilde{m}}$ for user $\tilde{u} \in \mathbb{U}$ can be detected by utilizing matched filtering as below:

$$\tilde{d}^{\tilde{u}}_{\tilde{k},\tilde{m}} = \Re\left\{ \theta^*_{\tilde{m},\tilde{k}} \sum_{n=-\infty}^{\infty} r[n] p^{\tilde{u}}_{\tilde{k}}\left[n - \frac{\tilde{m}}{\varepsilon_u}K\right]^* \right\}. \qquad (5)$$

Given the channel impulse response defined in (4), i.e. $r[n] = \sum_{u \in \mathbb{U}} s_u[n - \tau_u K] e^{-j\pi\nu_u \frac{n}{K}}$, and by application of the cross ambiguity function $A_{u\tilde{u}}(\tau, \nu)$ for two real-valued PFFs $p^u[n]$ and $p^{\tilde{u}}[n]$ according to

$$A_{u\tilde{u}}(\tau, \nu) = \sum_{n=-\infty}^{\infty} p^u[n] p^{\tilde{u}}[n - \tau K] e^{-j\pi\nu \frac{n}{K}}; \qquad (6)$$

with $\tau K \in \mathbb{Z}, \nu \in \mathbb{R}$, (5) can be rewritten according to

$$
\tilde{d}^{\tilde{u}}_{\tilde{k},\tilde{m}} = \Re\left\{ \sum_{u \in \mathbb{U}} \sum_{(m,k)} \theta^*_{\tilde{m},\tilde{k}} \theta_{m,k} d^u_{k,m} \right.
$$
$$
\left. \cdot \underbrace{\sum_{n=-\infty}^{\infty} p^u_k\left[n - \left(\frac{m}{\varepsilon_u} + \tau_u\right)K\right] p^{\tilde{u}}_{\tilde{k}}\left[n - \frac{\tilde{m}}{\varepsilon_{\tilde{u}}}K\right] e^{-j\pi\nu_u \frac{n}{K}}}_{A_{u\tilde{u}}\left(\frac{\tilde{m}}{\varepsilon_{\tilde{u}}} - \frac{m}{\varepsilon_u} - \tau_u, \tilde{k}\varepsilon_{\tilde{u}} - k\varepsilon_u\right) - \nu_u} \right\}.
$$
$$(7)$$

With the set $\mathbb{U}_c$ of coexisting users, $\tilde{\mathbb{K}}_u = \tilde{k} - \mathbb{K}_u$ and $\tilde{\mathbb{M}}_u = \tilde{m} - \mathbb{M}_u$, $\mu \in \tilde{\mathbb{M}}_u$ and $\kappa \in \tilde{\mathbb{K}}_u$ being the differences between the OQAM symbols and subcarriers, respectively, (7) can be split into a data and two different interference parts according to

$$
\tilde{d}^{\tilde{u}}_{\tilde{k},\tilde{m}} = \underbrace{\tilde{d}^{\tilde{u}}_{\tilde{k},\tilde{m}} A^{\Re}_{\tilde{u}\tilde{u}}(-\tau_{\tilde{u}}, -\nu_{\tilde{u}})}_{\text{data}}
$$
$$
+ \underbrace{\sum_{(\mu,\kappa)} d^{\tilde{u}}_{\tilde{k}-\kappa,\tilde{m}-\mu} A^{\Re}_{\tilde{u}\tilde{u}}\left(\frac{\mu}{\varepsilon_{\tilde{u}}} - \tau_{\tilde{u}}, \kappa\varepsilon_{\tilde{u}} - \nu_{\tilde{u}}\right)}_{\text{intrinsic interference, } u=\tilde{u}, (\mu,\kappa)\neq(0,0)},
$$
$$
+ \underbrace{\sum_{u \in \mathbb{U}_c} \sum_{(\mu,\kappa)} d^u_{\tilde{k}-\kappa,\tilde{m}-\mu} A^{\Re}_{u\tilde{u}}\left(\frac{\mu}{\varepsilon_u} - \mu_0 - \tau_u, \varepsilon_u\kappa - \kappa_0 - \nu_u\right)}_{\text{co-user interference, } \tilde{u}=\mathbb{U}\backslash\mathbb{U}_c},
$$
$$(8)$$
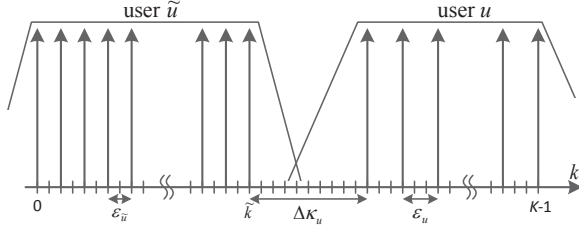
Fig. 2. Example of a two user scenario utilizing different subcarrier spacings with $\varepsilon_{\tilde{u}} = 2$ and $\varepsilon_u = 3$ and a guard band of $\Delta\kappa_u = 9$ subcarriers.

with

$$A_{u\tilde{u}}^{\Re}\left(\frac{\mu}{\varepsilon_u} - \tau_u, \varepsilon_u\kappa - \nu_u\right) = \Re\left\{\theta_{\kappa,\mu}^* A_{u\tilde{u}}\left(\frac{\mu}{\varepsilon_u} - \tau_u, \varepsilon_u\kappa - \nu_u\right)\right\},$$
$$(9)$$

and

$$\mu_0 = \left(\frac{\varepsilon_u}{\varepsilon_{\tilde{u}}} - 1\right)\frac{\tilde{m}}{\varepsilon_u}, \qquad (10)$$

$$\kappa_0 = \left(1 - \frac{\varepsilon_{\tilde{u}}}{\varepsilon_u}\right)\tilde{k}\varepsilon_u. \qquad (11)$$

In case of perfect time and frequency synchronization for user $\tilde{u}$, i.e. $\tau_{\tilde{u}} = \nu_{\tilde{u}} = 0$, and having an approximately perfect reconstruction performance of pulse $p^{\tilde{u}}[n]$, (8) reduces to

$$\tilde{d}_{\tilde{k},\tilde{m}}^{\tilde{u}} = \underbrace{\sum_{u \in \mathbb{U}_c} \sum_{(\mu,\kappa)} d_{\tilde{k}-\kappa,\tilde{m}-\mu} A_{u\tilde{u}}^{\Re}\left(\frac{\mu}{\varepsilon_u} - \Delta\mu_u, \varepsilon_u\kappa - \Delta\kappa_u\right)}_{\text{co-user interference}}$$
$$+ \underbrace{d_{\tilde{k},\tilde{m}}^{\tilde{u}} A_{\tilde{u}\tilde{u}}^{\Re}(0,0)}_{\text{data}}; \qquad (12)$$

$$\Delta\mu_u = \frac{\mu_0}{\varepsilon_u} + \Delta\tau_u; \quad \Delta\kappa_u = \kappa_0\varepsilon_u + \Delta\tau_u \qquad (13)$$

with $\Delta\tau_u = \tau_u - \tau_{\tilde{u}}$ and $\Delta\nu_u = \nu_u - \nu_{\tilde{u}}$ being the relative time delay and frequency offset between the received and co-existing users, respectively. Note that the amount of received co-user interference per OQAM symbol depends on the OQAM-OFDM symbol position $\tilde{m}$ within the transmission signal.

3. COEXISTENCE PERFORMANCE

The coexistence performance between spectrally adjacent users is measured by the signal-to-interference ratio ($SIR_{\tilde{u}}$), which determines the amount of intrinsic interference power σ_i^2 and the time and frequency offset dependent co-user interference $\sigma_c^2(\Delta\mu_u, \Delta\kappa_u)$ induced to the demodulated data of

$\tilde{d}_{\tilde{k},\tilde{m}}$ of power σ_s^2. This can be defined according to

$$SIR_{\tilde{u}}(\Delta\mu_u, \Delta\kappa_u) = \frac{\sigma_s^2}{\sigma_i^2 + \sigma_c^2(\Delta\mu_u, \Delta\kappa_u)}. \qquad (14)$$

According to (12), with the assumption of perfect time and frequency synchronization, the intrinsic interference is negligible and the $SIR_{\tilde{u}}$ can be rewritten as

$$SIR_{\tilde{u}}(\Delta\mu_u, \Delta\kappa_u) = \frac{\sigma_s^2}{\sigma_c^2(\Delta\mu_u, \Delta\kappa_u)}$$
$$= \frac{\sigma_s^2}{\sum\limits_{u \in \mathbb{U}_c} \sum\limits_{(\mu,\kappa)} \sigma_c^2(\mu, \kappa, \Delta\mu_u, \Delta\kappa_u)}, \quad (15)$$

where $\sigma_c^2(\mu, \kappa, \Delta\tau_u, \Delta\nu_u)$ denotes the co-user interference power induced by the OQAM symbol of user u with symbol and subcarrier offset μ and κ, respectively. Based on (12), statistically independent data symbols and with $\mathbb{E}\{|d_{k,m}|^2\} = 1/2$, the average energy $\sigma^2 = \mathbb{E}\{|\tilde{d}_{\tilde{k},\tilde{m}}|^2\}$ received per OQAM symbol can be obtained by

$$\sigma^2 = \underbrace{\frac{1}{2}\left|A_{\tilde{u}\tilde{u}}^{\Re}(0,0)\right|^2}_{\sigma_s^2}$$
$$+ \sum_{u \in \mathbb{U}_c} \sum_{(\mu,\kappa)} \underbrace{\frac{1}{2}\left|A_{u\tilde{u}}^{\Re}\left(\frac{\mu}{\varepsilon_u} - \Delta\mu_u, \varepsilon_u\kappa - \Delta\kappa_u\right)\right|^2}_{\sigma_c^2(\mu,\kappa,\Delta\mu_u,\Delta\kappa_u)}. \quad (16)$$

For the estimation of the coexistence performance it is our descision to analyze the worst case coexistence scenario for multi-user cases as depicted in Figure 2 and to evaluated the minimal SIR in a system. For this coexistence case of two users, κ_0 and μ_0 in (13) simplify by $\kappa_0 \in \{0, \ldots, \max(\varepsilon_u, \varepsilon_{\tilde{u}}) - 1\}$, denoting the integer subcarrier spacing offset between two users, and $\mu_0 \in \mathbb{M}_0 = \{0, \ldots, 2\varepsilon_u - 1\}/(\varepsilon_u\varepsilon_{\tilde{u}})$, denoting the fractional OQAM-OFDM symbol offset normalized to K, respectively. Accordingly, (15) can be rearranged to

$$SIR_{\tilde{u}}(\Delta\mu_u, \Delta\kappa_u) = \frac{\left|A_{\tilde{u}\tilde{u}}^{\Re}(0,0)\right|^2}{\sum\limits_{(\mu,\kappa)} \left|A_{u\tilde{u}}^{\Re}\left(\frac{\mu}{\varepsilon_u} - \Delta\mu_u, \varepsilon_u\kappa - \Delta\kappa_u\right)\right|^2}. \quad (17)$$

As mentioned in the previous section, the co-user interference depends on $\tilde{m}$. To evaluate the performance of different co-user scenarios, we define the time and frequency offset dependent mean SIR $\overline{SIR_{\tilde{u}}}(\Delta\tau_u, \Delta\kappa_u)$, which is given as follows

$$\overline{SIR_{\tilde{u}}}(\Delta\tau_u, \Delta\kappa_u) = \frac{1}{|\mathbb{M}_0|} \sum_{\mu_0 \in \mathbb{M}_0} SIR_{\tilde{u}}(\Delta\mu_u(\mu_0), \Delta\kappa_u). \quad (18)$$

(a) $\overline{SIR}_{\tilde{u}}(\Delta\tau_u, \Delta\kappa_u)$ of user $\tilde{u}$ for $\frac{\varepsilon_{\tilde{u}}}{\varepsilon_u} = \frac{1}{2}$ (b) $\overline{SIR}_u(\Delta\tau_u, \Delta\kappa_u)$ of user u for $\frac{\varepsilon_{\tilde{u}}}{\varepsilon_u} = \frac{1}{2}$ (c) $\min(\overline{SIR}_{\tilde{u}}(\Delta\tau_u, \Delta\kappa_u), \overline{SIR}_u(\Delta\tau_u, \Delta\kappa_u))$
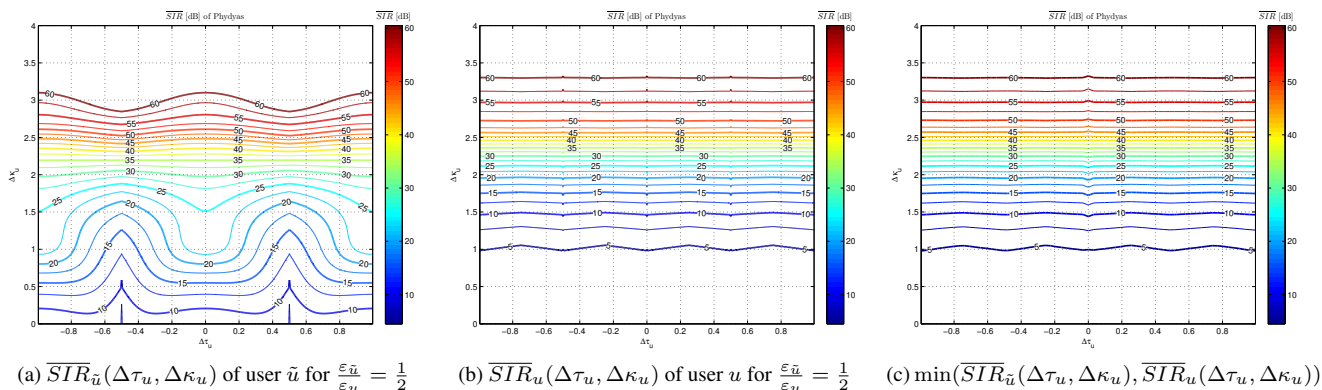
Fig. 3. $\overline{SIR}$ of a border subcarrier of a perfectly synchronized OQAM-OFDM system with $\varepsilon_{\tilde{u}}$ coexisting with an OQAM-OFDM system with ε_u and time offset $\Delta\tau_u$ as well as frequency offset $\Delta\kappa_u$, each utilizing a Phydyas PFF with overlapping factor $\gamma = 4$.

4. RESULTS

In this section, we quantify the coexistence performance for the scenario described in the previous section utilizing the Phydyas PFF [5] and IOTA PFF with spreading factor $\alpha = \{1, 2, 3\}$ [6] with an overlapping factor $\gamma = 4$, which have been suggested for FBMC systems, as well as different subcarrier spacing ratios $\varepsilon = \exp(|\ln(\varepsilon_{\tilde{u}}/\varepsilon_u)|)$. For this purpose the influence of synchronization errors on the amount of inflicted interference is investigated, followed by an assessment of the dimensioning of guard bands between different users. From system development and implementation point of view it is beneficial to limit the amount of different subcarrier spacing modes to minimize hardware costs. As subcarrier spacing ratios $\varepsilon = 2^x; x \in \mathbb{Z}$ can be implemented without reasonable hardware costs by implementation of a maximum size FFT, we restrict our investigations on this set of values. As currently deployed broadband mobile communication systems operating with a bandwidth of 5 MHz utilize 64 (802.11a) up to 512 (LTE) subcarriers, it is suitable to investigate $x = \{0, \ldots, 3\}$.

4.1. Synchronization robustness

For the evaluation of the synchronization error robustness, we analyze selected PFF and subcarrier spacing scenarios. Example $\overline{SIR}$ plots for a two user scenario utilizing the Phydyas PFF and a subcarrier spacing ratio $\varepsilon = 2$ undergoing time and frequency offsets are depicted in Figure 3. Therein Figure 3a depicts the $\overline{SIR}$ for the system with the smaller subcarrier spacing and Figure 3b the $\overline{SIR}$ of the one with the larger subcarrier spacing. Figure 3c shows the minimum SIR in the coexistence scenario between both systems. In Figure 4 the $\overline{SIR}$ performance for coexisting OQAM-OFDM systems utilizing the Phydyas and the EGF with $\alpha = 2$ PFFs is presented. From these results two different aspects for the coexistence performance of OQAM-OFDM systems can be deduced. First, the system utilizing the PFF with the highest
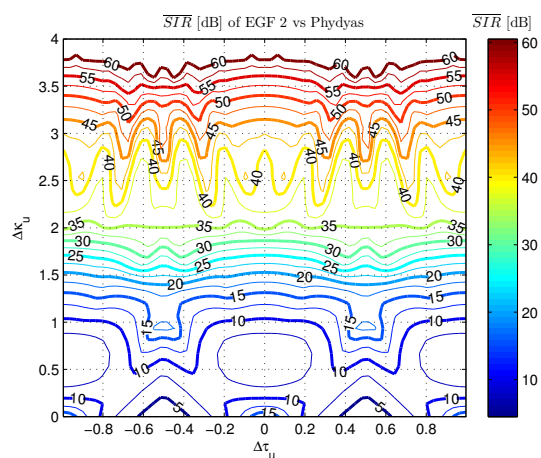
Fig. 4. Minimum $\overline{SIR}$ of a border subcarrier of a perfectly synchronized OQAM-OFDM system utilizing a Phydyas PFF coexisting with an OQAM-OFDM system utilizing a EGF PFF with $\alpha = 2$ and with a time offset $\Delta\tau_u$ as well as frequency offset $\Delta\kappa_u$.

energy spread in frequency domain mainly effects the minimum SIR within the coexisting scenario. This can be explained by the fact that the energy within a certain bandwidth collected from adjacent systems is the higher the larger the spread of the receiving PFF is. The second issue is the observed approximately timing offset independence of the SIR. This property proves OQAM-OFDM to be a potential candidate for application in asynchronous multi-service and MTC systems.

4.2. Guard band dimensioning

Besides the synchronization robustness it is mandatory to determine the required amount of virtual guard carriers Δk for target minimum SIR and maximum CFO $\Delta\nu_{u,\max} \geq |\Delta\nu_u|$ values in different coexistence scenarios. The guard carriers

	EGF 1	EGF 2	EGF 3	Phydyas
		$\Delta k = 1$		
EGF 1	29.5	18.3	14.4	31.4
EGF 2	20.3	15.7	12.8	20.2
EGF 3	16.0	13.4	11.3	15.8
Phydyas	30.0	18.1	14.2	32.6
		$\Delta k = 2$		
EGF 1	47.6	35.2	27.2	50.4
EGF 2	34.0	29.2	24.7	34.4
EGF 3	25.3	23.4	21.1	25.4
Phydyas	51.5	35.5	27.2	66.9
		$\Delta k = 4$		
EGF 1	51.6	53.3	46.9	53.5
EGF 2	54.8	56.6	45.2	64.1
EGF 3	45.5	44.1	39.3	46.0
Phydyas	55.4	65.0	47.5	84.9

Table 1. Maximum $\overline{SIR}$ [dB] achievable for a certain amount of guard carriers Δk taking a maximum carrier frequency offset $\Delta \nu_{u,\max} = 0.5$ into account. The left column holds the PFF of the receiver system and the top row the PFF of the coexisting one.

Δk in the virtual grid K can be calculated according to

$$\Delta k = \left\lceil \min_{SIR}(\Delta \kappa_u - \Delta \nu_{u,\max}) \right\rceil - 1, \qquad (19)$$

whereby $\Delta \kappa_u$ denotes the distance between both systems based on the virtual lattice grid. Table 1 holds the achievable SIR in dependence on the applied amount of virtual guard carriers Δk as well as the utilized PFFs for $\varepsilon = 1$ and $\Delta \nu_{u,\max} = 0.5$. The results indicate that for the investigated PFFs, an in-band guard band of one to two virtual guard carriers is suitable to attain a minimum interference isolation of more than 20 dB. The results for the coexistence of systems with different subcarrier spacings are summarized in Table 2. These results show that the relation between the required amount of virtual guard carriers is approximately linearly dependent on the applied ε, rendering possible a simple guard band dimensioning design rule.

5. CONCLUSION

In this contribution we quantitatively assessed the influence of channel adaptive modulation on the coexistence performance in the context of multi-user or multi-service scenarios. The simulation results prove that the required amount of guard bands for OQAM-OFDM systems is quasi-independent on the time offset between different users. As a rule of thumb we can state, that for a minimum interference isolation of 20 dB a bandwidth of one to two subcarrier spacings of the user with the largest subcarrier spacing has to be reserved for in-band guard bands. These results prove OQAM-OFDM to

	EGF 1	EGF 2	EGF 3	Phydyas
		$\Delta k = \varepsilon$		
$\varepsilon = 2$	4.6	3.9	3.2	4.6
$\varepsilon = 4$	4.6	2.8	1.7	4.5
$\varepsilon = 8$	4.8	2.1	0.8	4.5
		$\Delta k = 2\varepsilon$		
$\varepsilon = 2$	45.5	26.3	18.9	55.2
$\varepsilon = 4$	48.4	29.1	20.8	58.8
$\varepsilon = 8$	47.6	28.4	20.0	60.4
		$\Delta k = 4\varepsilon$		
$\varepsilon = 2$	52.8	58.7	42.0	84.0
$\varepsilon = 4$	54.0	59.6	42.1	84.7
$\varepsilon = 8$	54.9	58.2	40.7	84.0

Table 2. Maximum $\overline{SIR}$ [dB] achievable for a certain amount of virtual guard carriers Δk taking a maximum carrier frequency offset $\Delta \nu_{u,\max} = 0.5$ into account.

be a potential candidate for application in asynchronous and sub-band wise configured multi-service systems.

REFERENCES

[1] METIS, "Deliverable D2.1 - Requirement analysis and design approaches for 5G air interface," Tech. Rep., 2013.

[2] Ari Viholainen, Maurice Bellanger, and Mathieu Huchard, "Prototype filter and structure optimization," Tech. Rep., PHYDYAS, 2009.

[3] Malte Schellmann, Zhao Zhao, Hao Lin, Pierre Siohan, Nandana Rajatheva, Volker Luecken, and Aamir Ishaque, "FBMC-based air interface for 5G Mobile : Challenges and proposed solutions," in *Cognitive Radio Oriented Wireless Networks and Communications (CROWNCOM), 2014 9th International Conference on*, 2014, pp. 102–107.

[4] Martin Fuhrwerk, Jürgen Peissig, and Malte Schellmann, "Channel Adaptive Pulse Shaping For OQAM-OFDM Systems," in *Signal Processing Conference (EUSIPCO), 2014 Proceedings of the 22nd European*, 2014, pp. 181–185.

[5] Shahriar Mirabbasi and Ken Martin, "Design of prototype filter for near-perfect-reconstruction overlapped complex-modulated transmultiplexers," in *2002 IEEE International Symposium on Circuits and Systems. Proceedings (Cat. No.02CH37353)*. 2002, vol. 1, pp. I–821–I–824, IEEE.

[6] Pierre Siohan and Christian Roche, "Cosine-modulated filterbanks based on extended Gaussian functions," *IEEE Transactions on Signal Processing*, vol. 48, no. 11, pp. 3052–3061, 2000.